Nuclear Science and Techniques (2025) 36:30
https://doi.org/10.1007/s41365-024-01601-3

Implementation of a double trigger condition system based on charge comparison and TOF measurement for the NEDA detector array

J. M. Deltoro[1] · A. Goasduff[2] · F. J. Egea[1,2] · V. González[1] · A. Gadea[3] · R. M. Pérez-Vidal[2,3] · I. Lazarus[4] · M. Kogimtzis[4] · L. McNicholl[4] · M. Palacz[5] · G. Jaworski[5] · J. J. Valiente-Dobón[2] · J. Nyberg[6] · S. Casans[1] · A. E. Navarro-Antón[1] · E. Sanchis[1] · A. Boujrad[7] · E. Clément[7] · T. Hüyük[3] · R. Illicachi[3] · O. Stezowski[8] · V. Modamio[9]

Received: 17 April 2024 / Revised: 6 July 2024 / Accepted: 6 August 2024 / Published online: 11 January 2025

Abstract

The NEutron Detector Array (NEDA) is designed to be coupled to gamma-ray spectrometers to enhance the sensitivity of the setup by enabling reaction channel selection through counting of the evaporated neutrons. This article presents the implementation of a double trigger condition system for NEDA, which improves the acquisition of neutrons and reduces the number of gamma rays acquired. Two independent triggers are generated in the double trigger condition system: one based on charge comparison (CC) and the other on time-of-flight (TOF). These triggers can be combined using OR and AND logic, offering four distinct trigger modes. The developed firmware is added to the previous one in the Virtex 6 field programmable gate array (FPGA) present in the system, which also includes signal processing, baseline correction, and various trigger logic blocks. The performance of the trigger system is evaluated using data from the E703 experiment performed at GANIL. The four trigger modes are applied to the same data, and a subsequent offline analysis is performed. It is shown that most of the detected neutrons are preserved with the AND mode, and the total number of gamma rays is significantly reduced. Compared with the CC trigger mode, the OR trigger mode allows increasing the selection of neutrons. In addition, it is demonstrated that if the OR mode is selected, the online CC trigger threshold can be raised without losing neutrons.

Keywords Neutron detector · Neutron–gamma discrimination · Pulse shape analysis · Time-of-flight · Charge comparison

This work was supported by MICIU MCIN/AEI/10.13039/501100011033, Spain with Grant PID2020-118265GB-C42,-C44, PRTR-C17.I01, by Generalitat Valenciana, Spain with Grant CIPROM/2022/54, ASFAE/2022/031, CIAPOS/2021/114 and by the EU NextGenerationEU, ESF funds. This work was also supported by the National Science Centre (NCN), Poland (Grant No. 2020/39/D/ST2/00466).

✉ J. M. Deltoro
josemadeltoro@gmail.com

1 Department of Electronic Engineering, University of Valencia, Burjassot, Valencia, Spain

2 Istituto Nazionale di Fisica Nucleare, Laboratori Nazionali di Legnaro, Laboratori Nazionali di Legnaro, Legnaro, Padova, Italy

3 Instituto de Física Corpuscular, CSIC-Universidad de Valencia, CSIC-Universidad de Valencia, 46980 Paterna, Valencia, Spain

4 Science and Technology Facilities Council, Daresbury, UK

5 Heavy Ion Laboratory, University of Warsaw, 02-093 Warsaw, Poland

6 Department of Physics and Astronomy, Uppsala University, Uppsala, Sweden

7 Grand Accélérateur National d'Ions Lourds (GANIL), CEA/DRF-CNRS/IN2P3, CEA/DRF-CNRS/IN2P3, Caen, France

8 Université de Lyon, Université Lyon-1, CNRS/IN2P3, UMR5822, IP2I, IP2I, 4 Rue Enrico Fermi, 69622 Villeurbanne Cedex, France

9 Department of Physics, University of Oslo, 0316 Oslo, Norway

1 Introduction

The NEutron Detector Array (NEDA) [1] is a neutron detector based on a liquid scintillator that provides efficient neutron–gamma discrimination making use of the pulse-shape analysis and time-of-flight (TOF) information. It was designed to be coupled to gamma-ray spectrometers, aiming to improve the sensitivity of the setup by allowing the selection of the reaction channel using conditions on the number of detected neutrons [2, 3]. The NEDA is based on individual hexagonal cells filled with ~3.15 L of liquid scintillator (ELJEN EJ301). In its first implementation in 2018, the array comprised 54 NEDA detectors at forward angles and 42 Neutron Wall [4] detectors arranged as a ring close to 90° [1]. The array was coupled to the state-of-the-art gamma-ray array AGATA [5] at GANIL (France) [6, 7]. The charged particle detector array DIAMANT [8] complemented the setup. Digital electronics read out all detectors synchronized thanks to a common time-stamp distributed by the Global Trigger and Synchronization (GTS) system [9]. The EXOGAM2 [10] trigger processor was used to select the events using fold conditions on the AGATA and NEDA array within settable time-windows.

The neutron detectors of NEDA are sensitive to neutrons and X- and gamma rays. X-rays are largely suppressed by shielding the detectors, but this is not possible for the higher energy gamma rays without hindering the neutron detection efficiency. Therefore, neutron–gamma discrimination (NGD) methods are required to determine the nature of the detected radiation. Several pulse shape analysis (PSA) methods have been developed to perform NGD for a large number of organic liquid scintillators and photo-multiplier tubes [11–13]. They all benefit from the difference between the falling slope of the gamma-ray signal and that of the neutron signal. Due to the more significant population of triplet states in the scintillator, neutron-induced signals have a larger fraction of the total charge in the tail of the signal. This is caused by the decay mode of the molecular triplet states, which is mostly delayed fluorescence.

The most accurate analysis and discrimination is performed offline, that is, after the acquisition has been carried out. However, from the front-end electronics, the trigger requests are restricted online by trigger conditions in order to reduce the large number of prompt and uncorrelated gamma rays that can be acquired, thus significantly increasing the ratio of neutrons among all acquired events.

In the first version of the NEDA electronics, the trigger method implemented in the firmware at the level of the digital pre-processing was based on charge comparison (CC). This method generates a trigger based on the ratio between two values computed integrating two regions of the signal, as shown in Fig. 1. These are the fast component, containing the leading edge and the beginning of the falling edge (a few samples after the constant fraction discrimination (CFD) trigger), and the slow component, starting directly at the end of the fast component and extending along the pulse. If the ratio is above a certain threshold, the event is considered a neutron, whereas if it is below, the signal is considered a gamma ray. However, with this method, low-energy neutrons can be lost because the reduced number of scintillation photons reduce the sensitivity of the CC method.

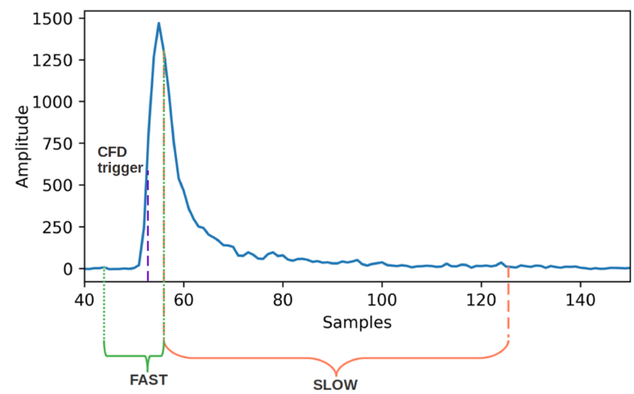

Fig. 1 (Color online) Slow and fast components of a pulse signal

For the purpose of acquiring low-energy neutrons, another trigger method based on TOF information could be used. In the electronic front-end of NEDA used during the 2018 campaign at GANIL, the TOF was measured as the time difference between an external logical signal, for example, the beam radio frequency signal (STOP), and the signal generated within the NEDA cell (START).

The addition of this trigger method allows for two independent trigger signals, which can then be combined. On the one hand, low-energy neutrons, which cannot trigger using a system based only on CC, can be acquired by using an OR logic of both trigger signals. On the other hand, these two trigger signals can be combined using an AND logic to reduce the high counting rate produced by a large number of gamma-ray events.

In this way, four trigger modes can be used in NEDA experiments depending on the pursued objectives, as follows:

- CC mode: Only the trigger generated by CC is used;
- TOF mode: Only the trigger based on TOF is considered;
- AND mode: A trigger signal is generated when both methods generate a trigger;
- OR mode: A trigger signal is generated when either of the two methods generates a trigger.

The rest of the paper is organized as follows. Section 2 presents the firmware description of the double trigger condition system. Section 3 describes the functional tests performed. Section 4 presents the results of the evaluation of the four trigger modes for the data of the E703 experiment at GANIL. Finally, in Sect. 5, the conclusions of this work are presented.

2 Firmware implementation

The main element of NEDA electronics at the 2018 campaign was the NUMEXO2 digitizer [14], which includes a Virtex 6 field programmable gate array (FPGA) and in addition a Virtex 5 FPGA that interfaces with the Global Trigger and Synchronization (GTS) [9] system and provides the data readout interfaces. The design of the new trigger system has been implemented in the Virtex 6 and uses, as inputs, the outputs of the trigger signals obtained independently. Given that the NUMEXO2 digitizer has 16 acquisition channels, this new functionality has been implemented independently for all the channels. The Virtex 6 firmware block diagram for one channel is shown in Fig. 2. It includes the blocks for the two trigger methods and the new double trigger block added. For the implementation of the new functionality, special care was taken to optimize the code and use the minimum possible FPGA resources due to the fact that it was already at 70% of its full capacity.

Following the signal path, the first firmware block is dedicated to the baseline cancelation and polarity inversion (leftmost on Fig. 2). In this block, the input samples come directly from the ADC mezzanines [15, 16], which digitize the detector signal at 200 Msps. Thanks to the dedicated registers, the users can set the baseline offset and signal polarity on a channel-by-channel basis.

At the output of this block, the baseline of the signal is subtracted, and the digital pulse of the detector becomes positive, independent of the original signal polarity. This output pulse is sent to three blocks: (1) leading edge, (2) digital constant fraction discriminator (DCFD), and (3) trigger block based on CC

The system can detect the arrival of an event in two ways. One way is in the leading edge block, where a boolean output signal is generated depending on whether the input pulse exceeds a certain threshold or not, indicating that a pulse has arrived. The other way is in the DCFD block, with the usual constant-fraction discriminator operation performed with configurable attenuation (K), delay, and threshold for each channel. From the DCFD, zero-crossover (ZCO) detection is used as a time reference signal, indicating the arrival of the pulse.

The same ZCO detection is used as a START signal for the TOF measurement using a time-to-digital converter (TDC) with the STOP coming from the accelerator radiofrequency signal.

The trigger block based on CC analyzes the signal generated in the detector to discriminate if the signal is a gamma ray or a neutron. To perform this, the algorithm carries out the following operation:

$$\text{Trigger if}: \quad \hat{I}_{\mathrm{s}} > \delta \cdot \hat{I}_{\mathrm{f}}, \tag{1}$$

where $\hat{I}_{\mathrm{s}}$ is the integral of the slow component of the input signal, $\hat{I}_{\mathrm{f}}$ is the integral of the fast component (see Fig. 1), and the δ is the threshold parameter, which can be adjusted using slow control (Fig. 2). The number of samples used to compute the fast and slow components can also be selected via slow control and are indicated by α and β values, respectively, in Fig. 2.

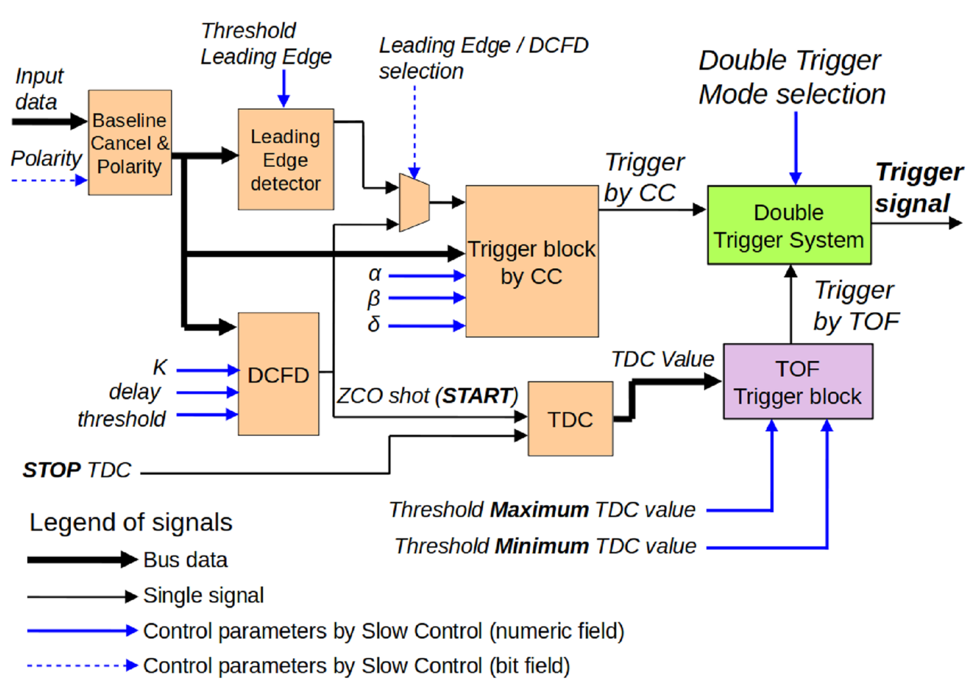

Fig. 2 (Color online) NUMEXO2 Virtex 6 firmware block diagram including the newly implemented double trigger block (green box) and the time-of-flight (TOF) trigger block (purple box). See text for details

The TDC block uses the measurement of the TOF between the ZCO detection signal and the accelerator radio-frequency external reference signal to generate a TDC value. This value is evaluated in the TOF trigger block (purple block in Fig. 2) where the trigger signal is activated when the TDC value lies between a lower (t_{MIN}) and upper (t_{MAX}) thresholds. These can be configured by the user through registers, following this expression:

$$\text{Trigger if}: \quad t_{MIN} < \text{TDC value} < t_{MAX} \tag{2}$$

Finally, the double trigger system block receives the trigger signals from the CC and TOF trigger methods. It generates the final trigger signal at its output according to the different discrimination modes.

To control the trigger modes and the corresponding thresholds, control parameters have been added to the slow control, modifying both the firmware and the slow control script. This design allows independent selection of trigger methods, CC thresholds, and TOF thresholds for each channel, providing greater flexibility.

The FPGA resources used in the implementation of the double trigger condition system only increased by 1%.

3 Functional test

The functional test aimed at testing the functionality of the double trigger implementation by evaluating the performance of the firmware for the different modes resulting from the combinations of the CC and TOF triggers. In particular, it was tested that the CC, TOF, AND, and OR trigger modes correctly discarded events outside the thresholds and maintained events within the established thresholds.

For the functional test, a ^{252}Cf source, with an activity of 610 KBq, was placed between a cylindrical BaF_2 detector, 2.54 cm in diameter and 2.54 cm in length, and a NEDA detector at a distance of 0.1 cm and 30 cm, respectively, as shown in Fig. 3. ^{252}Cf presents the advantage of being a mixed field-radiation source with a broad neutron energy distribution, similar to that observed in fusion evaporation reactions.

The NEDA signal was split in two using a linear fan-in fan-out (signal A in Fig. 3). One of the output signals was sent to the NUMEXO2 digitizer after passing through a single-ended to differential (SEDIFF) module to convert the unipolar signal into a differential signal. The second one was sent to an analog constant fraction discriminator (CFD Phillips 715), generating a logical NIM signal (signal B). An octal gate and delay generator (ORTEC GG8020) generated a coincidence window of 350 ns (signal C), setting the logic signal with the proper coincidence time width.

Fig. 3 (Color online) Test bench for the double trigger test

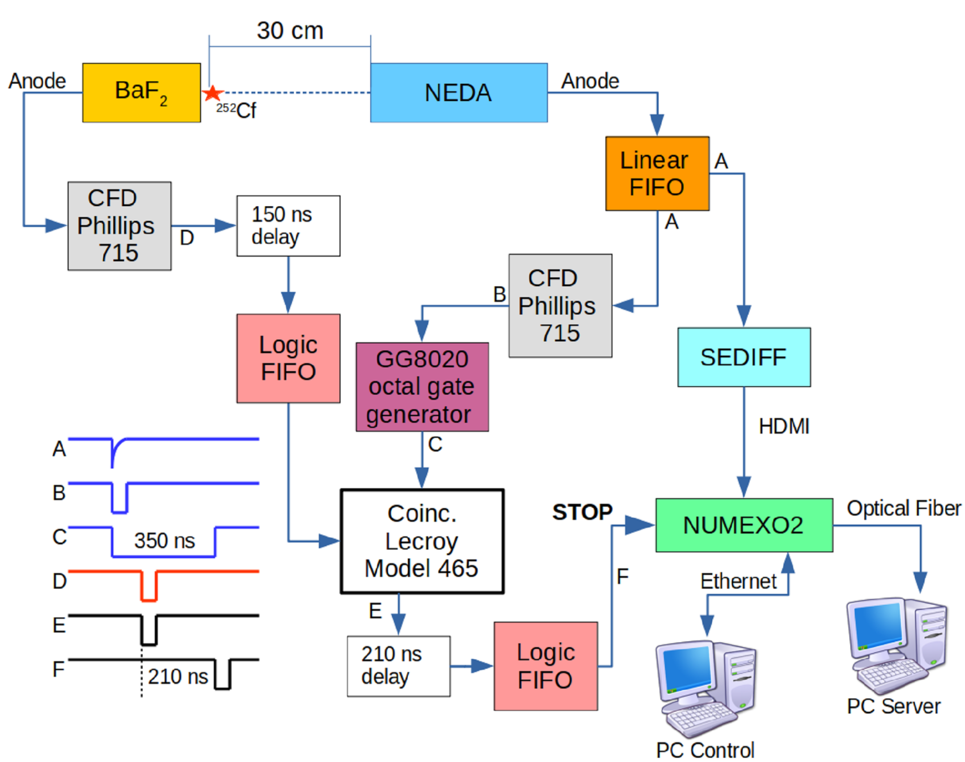

The BaF_2 signal passed through a CFD analog module to obtain a reference logic NIM signal (signal D). A coincidence unit (Lecroy 465) generated a logical NIM signal (signal E) when the NEDA and BaF_2 detectors were in coincidence. Due to the cable length and processing time within the NUMEXO2, this signal was obtained before the DCFD block had generated the START signal. Thus, it was necessary to delay it to have the STOP signal (signal F), which was driven into the NUMEXO2 to obtain the TDC value.

The NUMEXO2 sent the accepted signal, with the different trigger modes, through optical fibers to the data acquisition server. The different parameters of the slow control were controlled from a computer via Ethernet.

With this setup (Fig. 3), the modes of operation of the double trigger system were tested and the subfigures of Fig. 4 show the accepted events according to the results and thresholds of CC (Y-axis) and TOF (X-axis) calculated on the Virtex 6 FPGA. The thresholds used were 0.19 for CC and, from 135 to 225 for TOF.

Figure 4a shows the distribution of events in the case in which the thresholds allow accepting all events, that is, with no trigger condition. In Fig. 4b, it can be observed how a CC trigger condition prevents the acquisition of signals with lower δ than that programmed. Figure 4c shows the effect of applying the TOF trigger mode, in which events below the lower or above the upper thresholds are not acquired. Figure 4d shows the result of applying an AND condition to the CC and TOF triggers where only signals above a CC threshold and in a certain TOF range are accepted. Finally, in Fig. 4e, the result of the OR trigger mode is shown. In this case, the system rejects the signals below the CC threshold and out of the TOF range. All these results proved the correct functioning of the double trigger condition system with the described set-up.

4 In-beam results

After the functional verification, the double trigger condition system was verified using data collected in in-beam experiments. The impact of each trigger mode was evaluated after performing offline analysis and neutron–gamma discrimination. The analysis was focused on how the TOF, AND, and OR trigger modes affected the number of neutrons accepted after the offline PSA, compared with the case where only the CC online trigger mode was used.

For the purpose of evaluating the double trigger condition system, a specific dataset from experiment E703, with no trigger condition at the firmware level, was used. The E703 experiment, performed at GANIL with AGATA and the complementary NEDA, Neutron Wall, and DIAMANT instruments, aimed to study excited states above the 6^+ isomer in ^{102}Sn and ^{103}Sn using a ^{58}Ni beam impinging on

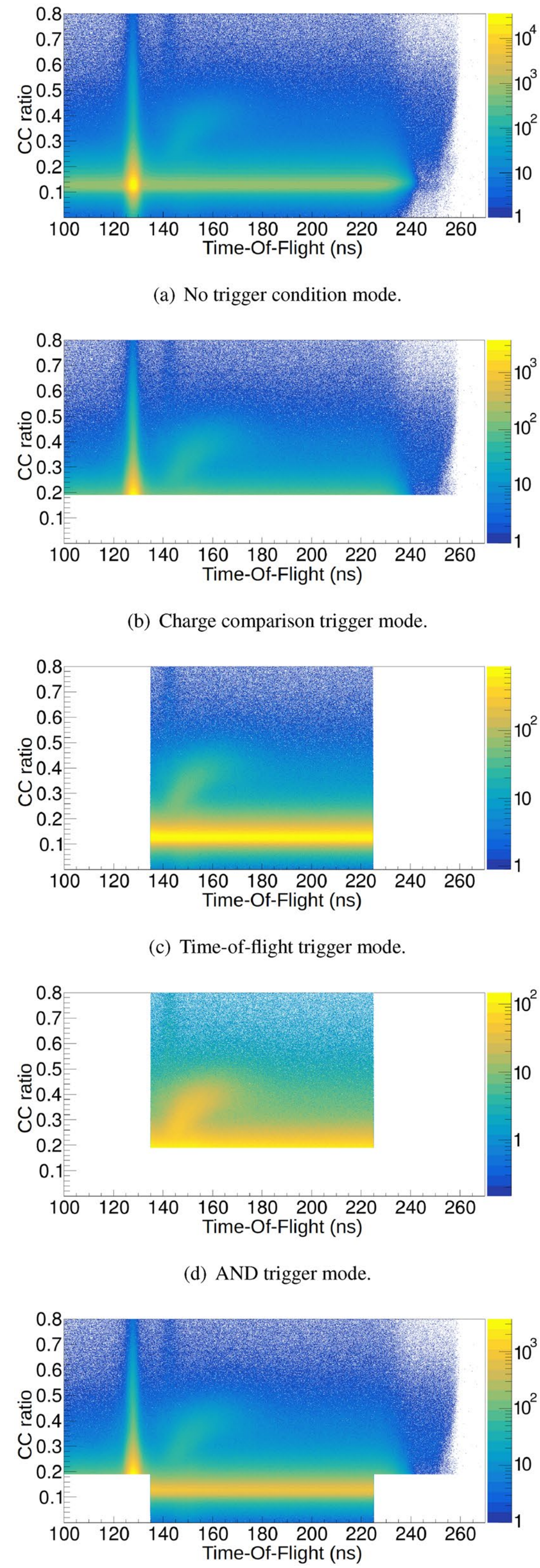

(a) No trigger condition mode.

(b) Charge comparison trigger mode.

(c) Time-of-flight trigger mode.

(d) AND trigger mode.

(e) OR trigger mode.

Fig. 4 (Color online) Functional test using the four trigger modes, and acquisition in the no trigger condition

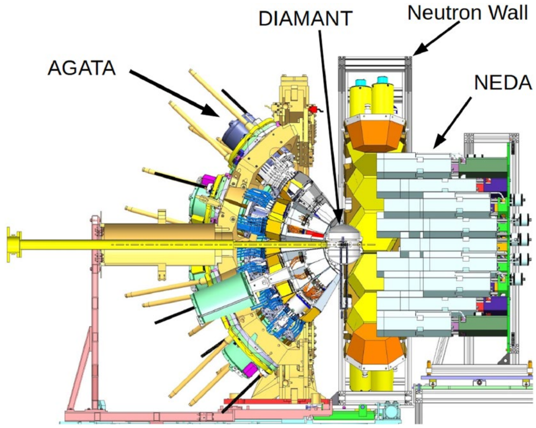

Fig. 5 (Color online) NEDA + AGATA + Neutron Wall + DIAMANT structure

a ^{50}Cr target at 200 MeV. Figure 5 shows the layout of the experimental setup.

The dataset contained events from all NEDA detectors with aligned offline CC and TOF information. This information was used to carry out the offline neutron–gamma discrimination. After this, the analyses of other datasets from the same experiment provided the proper selection zones (CUTs) for each type of event (neutron, prompt gamma, or uncorrelated gamma). Figure 6a shows the three regions: the black CUT encloses the neutrons, the red one the prompt gamma, and the yellow one the uncorrelated gamma. By counting the number of events in each CUT, we obtained the number of acquired events of each type. Figure 7a ("NO cond" column) shows the result of each integral in the no trigger condition. This result is used as a reference to compare the number of neutrons and gamma rays acquired with each trigger mode.

Next, the same process was carried out applying the four trigger modes simulating the trigger conditions that would have been applied in the trigger blocks at firmware level. The accepted events after the offline analysis are shown in Fig. 6b to e. The same CUTs were also applied and their integrals were calculated to obtain the number of events of each type.

The offline analysis employed improved the baseline removal techniques and the temporal information was more accurate owing to the use of interpolation techniques. This improved the pulse information obtained after offline analysis and was the reason why, after offline analysis, the CC ratio and TOF of some events differed from that calculated online in Virtex 6. Therefore, as shown in the subfigures in Fig. 6, some events appear outside the online trigger conditions (0.19 for the CC threshold, and from 135 to 225 for TOF thresholds).

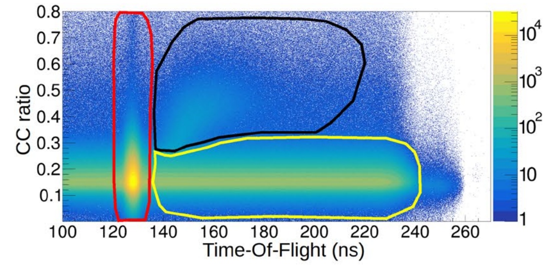

(a) No trigger condition.

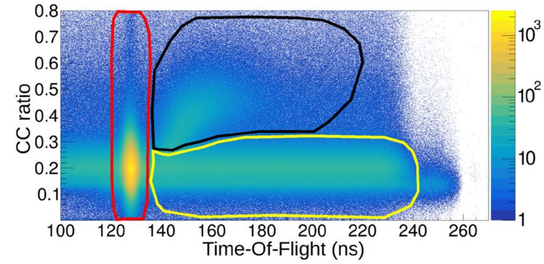

(b) Charge comparison trigger mode.

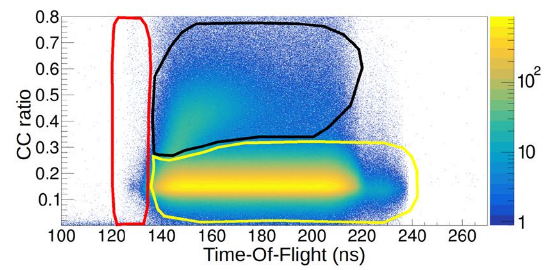

(c) Time-of-flight trigger mode.

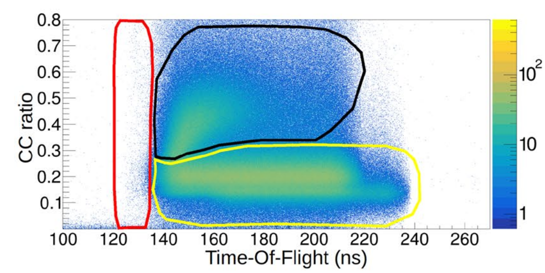

(d) AND trigger mode.

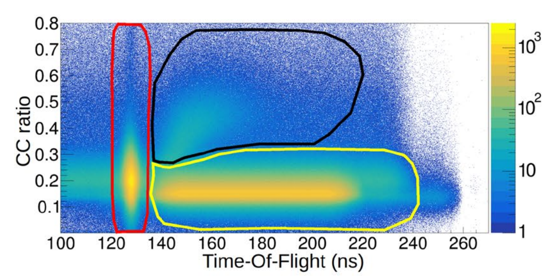

(e) OR trigger mode.

Fig. 6 (Color online) Events accepted after offline analysis in the no trigger condition and the four trigger modes with CC threshold at 0.19. Some events exceed the thresholds established at the firmware level due to the more accurate offline pulse shape analysis

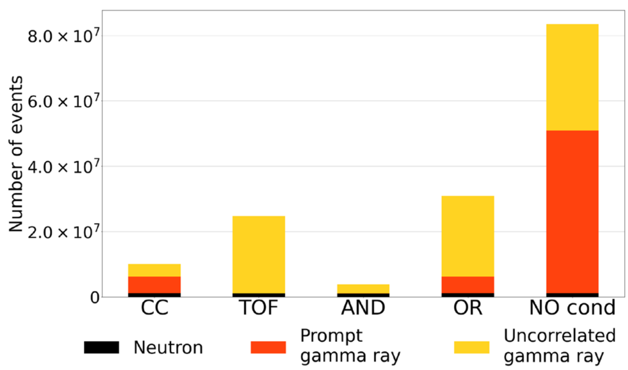

(a) Total events by trigger mode and total events in the no trigger condition.

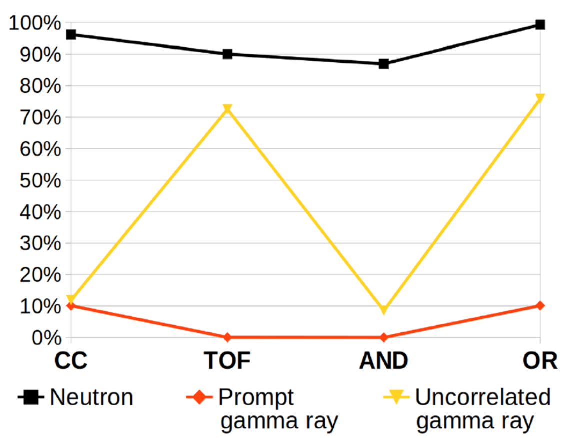

(b) Percentage by type of particle and by trigger mode compared with the no trigger condition.

Fig. 7 (Color online) **a** Total events acquired with each trigger mode. **b** Percentage of particles acquired compared with acquisition in the no trigger condition, taking into account the different trigger modes

Figure 7a shows the total events acquired in the no trigger condition and with each trigger mode, including the contribution of each type of event to the total, taking into account the integrals of each CUT after offline analysis. Figure 7b exhibits the percentage of accepted events compared with that in the case where no trigger condition is applied.

The first column of Fig. 7a shows the total number of events acquired with the CC trigger mode. A total of $1{\times}10^7$ events were acquired, representing as shown in Fig. 7b, 96.14% of the neutrons and reducing the prompt gamma rays and uncorrelated gamma rays to 10.10 and 11.89%, respectively, compared with the acquisition in the no trigger condition. The second column in Fig. 7a shows the results when a TOF trigger was used. It is shown that the number of events increases but the number of neutrons decreases compared with the CC trigger mode. However, we have a greater reduction (nearly to zero) of prompt gamma rays and a big increment in uncorrelated gamma-ray events.

For the AND condition, Fig. 7a shows that, compared with the CC trigger mode, the number of events acquired is reduced by up to 37.97%. This is because, with this trigger method, the trigger requests produced by prompt gamma rays were reduced to 0.01% compared with the case where no trigger condition was used, as shown in Fig. 7b. In addition, the number of neutrons acquired was reduced by 9.23% ($1{\times}10^5$ fewer neutron events) compared with those acquired with CC as a trigger mode, as seen in Fig. 7b.

The OR trigger mode, as shown in Fig. 7b, improved neutron acquisition by 3.11% (3×10^4 more neutron events) compared with the CC trigger mode. This trigger mode failed to reduce the trigger requests produced by uncorrelated gamma rays, thus increasing the total acquired events by 308.53% ($2{\times}10^7$ more events), as shown in Fig. 7a.

We also tested the influence of the CC threshold in the results of the different trigger modes. The TOF mode was not analyzed because the CC threshold had no impact in this case.

As shown in Fig. 8, with the CC and AND trigger modes, the percentage of accepted events was reduced as the CC threshold increased. For example, the percentage of neutrons with the AND trigger mode changed from 86.91 to 71.44% when the threshold changed from 0.19 to 0.3. Additionally, the percentage of prompt gamma rays

Fig. 8 (Color online) Percentage of particles acquired compared with acquisition in the no trigger condition. For the figure on the left, a CC threshold of 0.19 was used and for that on the right, 0.3

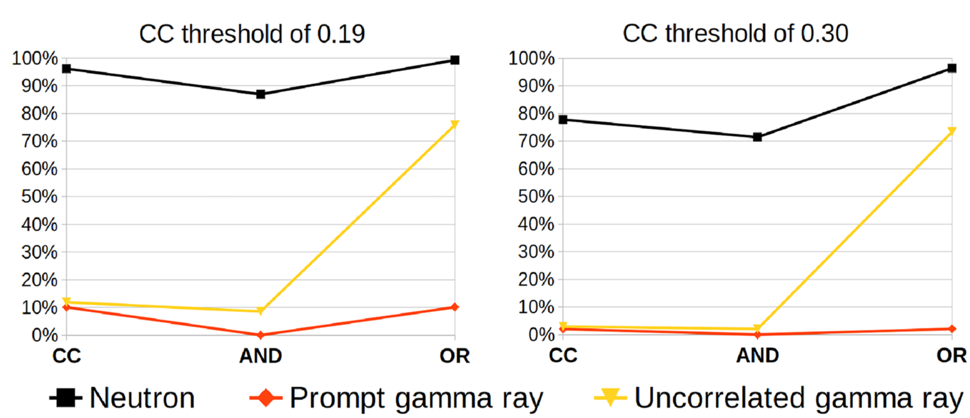

was reduced to 0%, and that of uncorrelated gamma rays was reduced from 8.56 to 2.08%.

Regarding the OR trigger mode, it was observed that the percentage of acquired neutrons only decreased by 2.87% (3×10^4 fewer neutron events) when comparing the results obtained using thresholds of 0.19 and 0.3. The prompt gamma rays were reduced by 8.05% (4×10^6 fewer gamma rays), and the uncorrelated gamma rays were reduced by only 2.49%.

5 Conclusion

After applying the four trigger modes on the data from the E703 experiment, we conclude that the AND trigger mode can be useful in experiments where the data acquisition system requires a low level of trigger request and it is not crucial to lose a small amount of neutron events. Further, it is shown that the OR trigger mode can be interesting in experiments where it is crucial to lose the minimum possible number of neutrons as long as the acquisition system can handle trigger requests at least three times higher than those using the CC trigger mode. Finally, the results of this work show that in experiments where it is necessary to increase the CC threshold, it will be necessary to use the OR mode of the trigger to avoid losing neutrons.

In conclusion, developing and implementing the double trigger condition system for the NEDA represents a significant advancement in enhancing the capabilities of spectrometry setups. Combining two independent trigger signals based on CC and TOF measurements, the NEDA array can effectively discriminate between gamma rays and neutrons, thus improving the precision and accuracy of reaction channel selection. The versatile trigger modes (CC, TOF, AND, and OR) offer researchers a range of options to tailor the detection system to their specific experimental goals. These trigger modes expand the range of detectable neutron energies and provide valuable flexibility in controlling the counting rates for various experimental scenarios. The firmware implementation using Virtex 6 FPGA and associated signal processing blocks demonstrates the feasibility of the proposed trigger system.

In the context of nuclear physics research, the NEDA detector array equipped with the double trigger condition system offers enhanced capabilities for precise reaction channel identification and data acquisition.

Acknowledgements We acknowledge the GANIL facility for the provision of heavy-ion beams as well as the AGATA, DIAMANT, and NEDA collaborations for instrumental support.

References

1. J.J. Valiente-Dobón, G. Jaworski, A. Goasduff et al., NEDA - NEutron Detector Array. Nucl. Instrum. Methods Phys. Res. A **927**, 81–86 (2019). https://doi.org/10.1016/j.nima.2019.02.021
2. G. Jaworski, M. Palacz, J. Nyberg et al., Monte Carlo simulation of a single detector unit for the neutron detector array NEDA. Nucl. Instrum. Methods Phys. Res. A **673**, 64–72 (2012). https://doi.org/10.1016/j.nima.2012.01.017
3. T. Hüyük, A. Di Nitto, G. Jaworski et al., Conceptual design of the early implementation of the NEutron Detector Array (NEDA) with AGATA. Eur. Phys. J. A **52**, 55 (2016). https://doi.org/10.1140/epja/i2016-16055-8
4. O. Skeppstedt, H.A. Roth, L. Lindström et al., The EUROBALL neutron wall - design and performance tests of neutron detectors. Nucl. Instrum. Methods Phys. Res. A **421**, 531–541 (1999). https://doi.org/10.1016/S0168-9002(98)01208-X
5. E. Clément, C. Michelagnoli, G. de France et al., Conceptual design of the AGATA 1π array at GANIL. Nucl. Instrum. Methods Phys. Res. A **855**, 1–12 (2017). https://doi.org/10.1016/j.nima.2017.02.063
6. G. Jaworski, A. Goasduff, F.J.E. Canet et al., The new neutron multiplicity filter Neda and its first physics campaign with Agata*. Acta Phys. Pol. B **50**, 585–590 (2019). https://doi.org/10.5506/APhysPolB.50.585
7. S. Akkoyun, A. Algora, B. Alikhani et al., AGATA-Advanced GAmma Tracking Array. Nucl. Instrum. Methods Phys. Res. A **668**, 26–58 (2012). https://doi.org/10.1016/J.NIMA.2011.11.081
8. J.N. Scheurer, M. Aiche, M.M. Aleonard et al., Improvements in the in-beam γ-ray spectroscopy provided by an ancillary detector coupled to a Ge γ-spectrometer: the DIAMANT-EUROGAM II example. Nucl. Instrum. Methods Phys. Res. A **385**, 501–510 (1997). https://doi.org/10.1016/S0168-9002(96)01038-8
9. M. Bellato, D. Bortolato, J. Chavas et al., Sub-nanosecond clock synchronization and trigger management in the nuclear physics experiment AGATA. J. Instrum. **8**, P07003 (2013). https://doi.org/10.1088/1748-0221/8/07/P07003
10. J. Simpson, F. Azaiez, G. de France et al., The EXOGAM array: a radioactive beam gamma-ray spectrometer. Acta. Phys. Hung. New Ser. Heavy Ion **11**, 159–188 (2000)
11. X.L. Luo, V. Modamio, J. Nyberg et al., Test of digital neutron-gamma discrimination with four different photomultiplier tubes for the NEutron Detector Array (NEDA). Nucl. Instrum. Methods Phys. Res. A **767**, 83–91 (2014). https://doi.org/10.1016/j.nima.2014.08.023
12. P.A. Söderström, G. Jaworski, J.J. Valiente-Dobón et al., Neutron detection and γ-ray suppression using artificial neural networks with the liquid scintillators BC-501A and BC-537. Nucl. Instrum. Methods Phys. Res. A **916**, 238–245 (2019). https://doi.org/10.1016/j.nima.2018.11.122
13. X. Fabian, G. Baulieu, L. Ducroux et al., Artificial neural networks for neutron/γ discrimination in the neutron detectors of NEDA. Nucl. Instrum. Methods Phys. Res. A **986**, 164750 (2021). https://doi.org/10.1016/j.nima.2020.164750
14. F.J. Egea Canet, C. Houarner, A. Boujrad et al., Digital front-end electronics for the neutron detector NEDA. IEEE Trans. Nucl. Sci **62**, 1063–1069 (2015). https://doi.org/10.1109/TNS.2015.2392159
15. F.J. Egea, E. Sanchis, V. González et al., Design and test of a high-speed flash ADC mezzanine card for high-resolution and timing performance in nuclear structure experiments. IEEE Trans. Nucl. Sci. **60**, 3526–3531 (2013). https://doi.org/10.1109/TNS.2013.2281241

16. F.J. Egea Canet, V. González, M. Tripon et al., A new front-end high-resolution sampling board for the new-generation electronics of EXOGAM2 and NEDA detectors. IEEE Trans. Nucl. Sci. **62**, 1056–1062 (2015). https://doi.org/10.1109/TNS.2015.2433021